Amino Acids (2014) 46:1907–1917
DOI 10.1007/s00726-014-1745-8

ORIGINAL ARTICLE

Glycine modulates membrane potential, cell volume, and phagocytosis in murine microglia

Barbara Komm · Marlena Beyreis · Michael Kittl · Martin Jakab · Markus Ritter · Hubert H. Kerschbaum

Received: 19 November 2013 / Accepted: 5 April 2014 / Published online: 24 April 2014

Abstract Phagocytes form engulfment pseudopodia at the contact area with their target particle by a process resembling cell volume (CV) regulatory mechanisms. We evaluated whether the osmoregulatory active neutral amino acid glycine, which contributes to CV regulation via activation of sodium-dependent neutral amino acid transporters (SNATs) improves phagocytosis in isotonic and hypertonic conditions in the murine microglial cell line BV-2 and primary microglial cells (pMG). In BV-2 cells and pMG, RT-PCR analysis revealed expression of SNATs (Slc38a1, Slc38a2), but not of GlyRs (Glra1–4). In BV-2 cells, glycine (5 mM) led to a rapid Na^+-dependent depolarization of membrane potential (V_{mem}). Furthermore, glycine increased CV by about 9 %. Visualizing of phagocytosis of polystyrene microspheres by scanning electron microscopy revealed that glycine (1 mM) increased the number of BV-2 cells containing at least one microsphere by about 13 %. Glycine-dependent increase in phagocytosis was suppressed by the SNAT inhibitor α-(methylamino)isobutyric acid (MeAIB), by replacing extracellular Na^+ with choline, and under hypertonic conditions, but not by the GlyR antagonist strychnine or the GlyR agonist taurine. Interestingly, hypertonicity-induced suppression of phagocytosis was rescued by glycine. These findings demonstrate that glycine increases phagocytosis in iso- and hypertonic conditions by activation of SNATs.

Keywords Cell volume regulation · Phagocytosis · Microglia · Glycine · SNAT

B. Komm · M. Kittl · H. H. Kerschbaum (✉)
Department of Cell Biology, University of Salzburg, Hellbrunnerstr. 34, 5020 Salzburg, Austria
e-mail: Hubert.Kerschbaum@sbg.ac.at

M. Beyreis · M. Kittl · M. Jakab · M. Ritter
Institute of Physiology and Pathophysiology, Paracelsus Medical University, 5020 Salzburg, Austria

M. Ritter
Gastein Research Institute, Paracelsus Medical University, 5020 Salzburg, Austria

Introduction

Glycine covers a broad spectrum of cellular homeostatic functions. In the central nervous system, it acts as an inhibitory neurotransmitter and contributes to the regulation of cell membrane potential. Moreover, it acts as organic osmolyte (Lang et al. 1998; Yancey 2005) and participates in cell volume regulation (Brocker et al. 2012; Dutertre et al. 2012; Franchi-Gazzola et al. 2006; Lang et al. 1998; Schiöth et al. 2013). Cells continuously adapt to osmotic stressors, evoked either by changes in osmolarity in their cellular environment, like osmotic gradients in the kidney or by changes in intracellular osmolarity due to metabolic activity, like synthesis or degradation of glycogen in the liver (Lang et al. 1993, 1998; Schliess and Häussinger 2003). Hypotonic environment provokes cell swelling, followed by a regulatory volume decrease (RVD) driven by cellular exit of osmolytes, whereas hypertonic conditions cause cell shrinkage followed by a regulatory volume increase (RVI) caused by osmolyte entry into the cell. Whereas RVD is associated with outward movement of K^+ ions and anions like HCO_3^- or Cl^-, RVI is mainly driven by cellular import of Na^+ via secondary active ion transporters including the sodium-dependent neutral amino acid transporters (SNATs) (Franchi-Gazzola et al. 2006; Hoffmann et al. 2009; Lang et al. 1998; Tramacere et al. 1984). Substrates of neutral amino acid transporters are proline, glutamine, alanine, methionine, serine and glycine. Among these substrates,

glycine is of particular interest, because it activates a Cl^- conductance when it binds to glycine receptors (GlyRs), but a Na^+ conductance when it binds to SNATs (Dutertre et al. 2012; Mackenzie and Erickson 2004; Schilling and Eder 2004). As inhibition of Cl^- conductance suppresses formation of engulfment pseudopodia, local extension of the plasma membrane embracing target particles and uptake of polystyrene microspheres, we suggested previously that phagocytosis is tightly linked to cellular volume regulation (Harl et al. 2013). Accordingly, we evaluated whether the organic osmolyte glycine has comparable consequences on phagocytosis.

Microglial cells are monocyte-derived cells in the brain that remove cell debris and pathogens in brain tissue (Kreutzberg 1996). Glycine-dependent effects in monocytes, like macrophages, Kupffer cells in the liver, or microglial cells in the brain, are either attributable to GlyRs or SNATs. Hyperpolarization of the cell membrane potential (V_{mem}) in Kupffer cells (Wheeler et al. 1999) are related to activation of GlyRs. Interestingly, glycine has also GlyR-independent, but SNAT-dependent effects. Glycine depolarizes V_{mem} in the microglial cell line BV-2. The glycine-induced current in BV-2 cells is insensitive to the GlyR antagonist strychnine, is not induced by the GlyR agonist taurine, is insensitive to changes in extracellular Cl^-, but sensitive to changes in extracellular Na^+ concentration and is inhibited with α-(methylamino)isobutyric acid (MeAIB), a specific substrate of SNATs (Schilling and Eder 2004). Similarly, Van den Eynden and colleagues showed that glycine and its precursor, L-serine, increased intracellular calcium transients in microglial cells that are insensitive to strychnine and taurine, but significantly decreased in the presence of the SNAT substrate, 2-aminoisobutyric acid (AIB) (Van den Eynden et al. 2011). Whereas GlyR mRNA and protein have been detected in Kupffer cells and macrophages (Froh et al. 2002), the expression of GlyR in microglial cells has not been evaluated directly.

The influence of glycine on phagocytosis is controversially discussed. In blood monocytes, glycine administration decreased *E. coli* phagocytosis at high concentrations (10 mM), but had no influence at lower concentrations (Spittler et al. 1999). In peritoneal macrophages, glycine (1 mM) has been reported to influence particle uptake positively. Glycine-dependent increase in myelin uptake was not affected by the GlyR antagonist strychnine or its agonist taurine. Moreover, the augmentation in phagocytosis was inhibited in the presence of AIB, alluding SNAT to be responsible for glycine-induced increase of phagocytosis in peritoneal macrophages (Carmans et al. 2004).

Understanding the effects of glycine on cellular homeostasis is relevant in the interpretation of the anti-inflammatory impact of glycine at the systemic level. Intravenous administration of glycine preceding surgery has been reported to diminish postoperative inflammatory ileus (Stoffels et al. 2011) and to reduce reperfusion injury, like hypoxia, necrosis and production of inflammatory cytokines in the donor of a liver transplant (Schemmer et al. 1999). Moreover, glycine reduces myocardial infarct size (Horwitz et al. 1994). Dietary glycine raises animal survival after endotoxin (LPS) shock and decreases liver necrosis and lung injury (Ikejima et al. 1996), diminishes cyclosporine A-induced kidney damages by decreasing necrosis and infiltration of macrophages and neutrophils (Thurman et al. 1997), has anti-inflammatory properties after endotoxin shock by decreasing the production and release of inflammatory cytokines, such as interleukin-1β (IL-1β) and tumor necrosis-factor α (TNF-α). In addition, glycine diminishes cyclosporine A-induced hypoxia and decreases formation of free radicals in rats (Zhong et al. 1998). Furthermore, there is strong evidence that glycine decreases cancer formation triggered by non-genotoxic carcinogens by decreasing cell proliferation and by reducing tumor volume as well as tumor vascularization (Wheeler et al. 1999). Interestingly, its administration before chemotherapy blunts chemotherapy-induced liver damage and diminishes inducible nitric oxide synthase (iNOS) expression (Mikalauskas et al. 2011). Critically, inflammatory processes are associated with hypertonic conditions in the microenvironment and interestingly, osmolytes suppress expression of pro-inflammatory factors (Brocker et al. 2012).

We have recently demonstrated that swelling-activated Cl^- conductance is associated with engulfment of polystyrene microspheres (Harl et al. 2013) in the microglia cell line BV-2 and primary microglial cells (pMG). In the present study, we asked whether the organic osmolyte glycine has an impact on microsphere uptake and cellular volume regulation in normo- and hypertonic conditions in these cells. We examined this issue by analyzing glycine-dependency of cell volume, cell membrane potential, ion conductance and uptake of polystyrene microspheres. Furthermore, we performed RT-PCR to identify GlyRs and SNATs. Our study demonstrates that (1) both BV-2 cells and pMG express SNATs (Slc38a1 and Slc38a) but no GlyRs (GlyR1, GlyR2, GlyR3, GlyR4); that (2) glycine evokes a system A-dependent Na^+ conductance; (3) increases cell volume; (4) facilitates phagocytosis in isotonic conditions and (5) rescues hypertonicity-induced suppression of phagocytosis.

Materials and methods

Cell culture

Primary microglial cells were isolated from forebrains of 1- to 3-day-old wild-type C57 black 6J mice (Hoffmann et al. 2007). Mice were killed by decapitation. After dissociation

of brain tissue with trypsin for 30 min at 37 °C and mechanical dissociation by centrifugation, microglia were co-cultivated with astrocytes in poly-D-lysine (PDL)-coated 75-cm^2 tissue culture flasks in Dulbecco's modified Eagle's medium (DMEM) supplemented with 10 % fetal calf serum (FCS; Gibco/BRL Life Technologies, MD, USA) and 1 % penicillin/streptomycin (Gibco). Six to nine animals were used per cell culture. After 10–14 days in culture at 37 °C and 5 % CO_2, pMG were harvested by vigorous shaking from an astrocyte monolayer for 3 h. The supernatant containing >97 % microglia was used for experiments. Adult wild-type C57 black 6J mice were ordered from and bred in the local animal housing at the University of Salzburg. Animal handling was performed according to Austrian law and approved by local authorities.

The murine microglial cell line BV-2 was cultured in 25-cm^2 tissue culture flasks in DMEM containing 2,200 mg/L glucose supplemented with 10 % FCS at 37 °C in a humidified atmosphere at 5 % CO_2. Twice a week cells were split and supplied with new medium. For experiments, BV-2 cells were removed from tissue culture flasks by treatment with 1 ml trypsin for 3 min. Afterwards, cell suspension was transferred into a centrifugation tube containing 8 ml DMEM (with 10 % FCS) and centrifuged at 200 g for 5 min. Microglial cells were resuspended in 1 ml DMEM (with 10 % FCS) and seeded into Petri dishes (diameter 3.5 cm) on poly-D-lysine (PDL)-coated (0.01 %) glass coverslips (diameter 12 mm) at a density of 6×10^4 cells/ml. Cells were incubated in a humidified atmosphere for up to 18 h to promote adhesion. Following two washing steps, cells were treated with different reagents in corresponding extracellular solution.

Reagents and solutions

Red fluorescent sulfate polystyrene microspheres (2 % solids, diameter 4 μm) were obtained from Invitrogen (Life Technologies, Vienna, Austria). DMEM medium and FCS for culture of microglial cells were from Sigma-Aldrich (St. Luis, Missouri, USA). Concentrations of amino acids in DMEM relevant for SNATs are (in g/L): glutamine 0.584, methionine 0.03, serine 0.042, glycine 0.03. Extracellular saline (Ringer) contained (in mM): NaCl 130, KCl 5, $CaCl_2$ 2, $MgCl_2$ 1, HEPES 10, D-glucose 8, titrated to pH 7.4 with NaOH. Cl^--free extracellular solution contained (in mM): Na-D-gluconate 130, K-D-gluconate 5, Ca-D-gluconate monohydrate 2, $MgSO_4$ 1, HEPES 10, D-Glucose 8, titrated to pH 7.4 with NaOH. Na^+-free solution contained (in mM): choline-chloride 130 mM, KCl 5, $CaCl_2$ 2, $MgCl_2$ 1, HEPES 10, D-glucose 8, titrated to pH 7.4 with NaOH. Phosphate buffered saline (PBS) contained (in mM): NaCl 150, KH_2PO_4 2, Na_2HPO_4 6.4, titrated to pH 7.4 with NaOH. 0.3, 1.0, 5.0 and 10.0 mM glycine were added to saline before the experiments. Experiments lasting 1 h were performed in extracellular saline, but experiments lasting 6 h were performed in DMEM (without serum). DMEM contained 400 μM glycine. Hypertonic solution (400 mosmol/L) was adjusted by addition of sucrose to serum-free DMEM and osmolarity was checked by freezing point depression (OM802; Vogel, Giessen, Germany). Absence or presence of glycine did not affect cell viability based on a trypan blue exclusion assay. All chemicals were purchased from Sigma-Aldrich (St. Louis, Missouri, USA). The reagents were prepared as stock solutions and stored at −20 °C until use. The drying solution hexamethyldisiloxane (HMDS) was from Merck (Vienna, Austria).

Scanning electron microscopy

For scanning electron microscopy (SEM), microglial cells were seeded on PDL-coated glass coverslips (diameter 12 mm) placed in a petri dish at a density of 6×10^4 cells. The petri dish was filled with DMEM (with 10 % FCS) and cells were allowed to adhere overnight in a humidified atmosphere at 37 °C and 5 % CO_2.

Phagocytic activity of microglial cells was evaluated using microspheres (3.41×10^6 microspheres/2 ml solution) in the absence and presence of reagents at 37 °C and 5 % CO_2. Cells were washed with extracellular solution and PBS, fixed in 2.5 % glutaraldehyde at room temperature for 1 h, washed in PBS overnight, dehydrated in an ethanol series (50–70–80–90–96–100–100–100 %) for 5 min each and air dried using HMDS two times for 10 min each. Then, coverslips were attached with lightening silver on SEM-stubs and covered with gold (Agar Sputter Coater). Microglial cells were observed using a Cambridge Stereoscan 250 scanning electron microscope. Electron micrographs were digitized and analyzed via orion software (ORION, Belgium).

Reverse-transcriptase (RT) PCR

Total RNA from BV-2 and pMG was extracted using the NucleoSpin® RNA II preparation kit (Macherey-Nagel). Total RNA from the spinal cord of 4-day-old mice, used as positive control, was extracted with RNAbee reagent (AMS biotechnology) based on phenol/chloroform extraction and isopropanol precipitation. 1 μg of isolated RNA was used for the reverse-transcriptase (RT) reaction with RevertAid Premium Reverse Transcriptase, RiboLock RNase inhibitor and oligo-dT18 primers (Thermo Scientific). The cDNA was applied to PCR (35 cycles, annealing temperature 60 °C) with specific primers for the mouse glycine receptor alpha subunit isoforms 1–4 (Glra1–4) and mouse sodium-coupled amino acid transporters (members

Table 1 Primers used for RT-PCR of mouse glycine receptor (GlyR) and sodium-coupled neutral amino acid transporter (SNAT) alpha subunit isoforms Glra1–4 and Slc38a1, 2 and 4, respectively

Target	GenBank®	Sequence (5′–3′)	Strand	Binding position	Size (bp)
Glra1	NM_020492	AGTTTCGGTTCCATCGCTGA	+	280–299	266
		GTCAGGGTGATTCTGATGCTGT	–	545–524	
Glra2	NM_183427	TCCCTCGCAGACCCTATCTC	+	223–242	170
		CTCGGTAGTCCATGGTGGTT	–	392–373	
Glra3	NM_080438	CACTGTTACTGAGTTTGGTGGC	+	138–159	206
		AGTCGTCTCTGCAATGGAGC	–	343–324	
Glra4	NM_010297	GCCTCTTTGCCTAAGGTGTC	+	934–953	207
		GCCACGAAAATAGAAGCGGC	–	1,140–1,121	
Slc38a1 transcript variants 1–3	NM_134086 NM_001166456 NM_001166458	GAGCTCAAAGACCGGTCACA	+	1,887–1,906, 1,194–1,213, 1,401–1,420	229
		TGAAAAACAGCACAGGCACG	–	2,115–2,096 1,422–1,403 1,629–1,610	
Slc38a2	NM_175121	TGTACTTGCTCGCTGCTCTC	+	1,382–1,401	180
		CGGAACTCCGGATAGGGAAA	–	1,561–1,542	
Slc38a4	NM_027052	TCCAACCCGAAGAGGGTAGA	+	72–91	275
		AGTCATTCCAGGGTGATGCTC	–	346–326	
Actb (β-actin)	NM_007393	ACCCGCCACCAGTTCGCCAT	+	62–81	311
		GGGGCCACACGCAGCTCATT	–	372–353	

Target genes, GenBank® accession numbers, primer sequences and orientation, binding positions on the mRNAs and amplicon sizes (bp, base pairs) are specified

1, 2 and 4 of solute carrier family 38; Slc38a1, 2 and 4), as listed in Table 1. β-Actin (Actb) served as internal (loading) control. PCR reactions were separated on 2 % agarose gels and visualized by Midori Green (NIPPON Genetics) staining. A 50-bp DNA Ladder was used as a size marker (GeneRuler, Thermo Scientific).

Electrophysiology

Cells were cultured in DMEM medium on poly-D-lysine-coated glass coverslips (1 cm Ø) and used for patch clamp experiments after 1–3 days. Coverslips were transferred to an RC-25 recording chamber (Warner Instruments) and mounted on an Olympus IMT-2 inverted microscope. V_{mem} recordings were performed in the whole-cell perforated patch clamp configuration in zero-current clamp mode. Data were acquired using an EPC-10 amplifier controlled by PatchMaster software (HEKA). Patch electrode resistances were 3–5 MΩ. Recordings were started, when series resistance was <30 MΩ. Data were analyzed with FitMaster software (HEKA) and Igor Pro 6 (WaveMetrics). Intracellular solution contained (in mM) 70 K_2SO_4, 10 NaCl, 10 KCl, 4 $MgCl_2$, 2 $CaCl_2$, 5 HEPES free-acid, 10 EGTA, 40 D-(+)-raffinose and 120 μg/ml amphotericin B (pH 7.2 adjusted with KOH) (296 mOsm/kg). Standard (control) extracellular solution contained (in mM) 140 NaCl, 5.6 KCl, 1.5 $MgCl_2$, 2.5 $CaCl_2$, 10 HEPES free-acid, 4.5 D-glucose and 5 mannitol (pH 7.4 adjusted with NaOH). Osmolality of intra- and extracellular solutions measured using a vapor pressure osmometer (Wescor) was 296 mOsm/kg. Bath solution exchange was done with a valve controlled gravity-driven perfusion system (ALA Scientific Instruments) at a flow rate of 3–5 ml/min. To assess glycine-driven cell membrane depolarizations, mannitol in the extracellular solution was iso-osmotically replaced by 0.3, 1, or 5 mM glycine. To disclose the Na^+-dependence of cell membrane depolarization in presence of 5 mM glycine, an extracellular solution was used in which NaCl was replaced by choline-chloride. Glycine-evoked inward currents were measured at a holding potential of −60 mV. All patch clamp experiments were performed at room temperature.

Assessment of the mean cell volume (MCV) by flow cytometry

Subconfluent BV-2 cells, grown under standard cell culture conditions for 4–5 days, were harvested by Trypsin/EDTA treatment and centrifuged for 5 min at 200×g. To measure the effects of 5 mM extracellular glycine on BV-2 cell volume, the cell pellet was resuspended in 3 ml (0.5–1.0 × 10^6 cells/ml) of extracellular solution containing (in mM) 140 NaCl, 5.6 KCl, 1.5 $MgCl_2$, 2.5 $CaCl_2$, 10 HEPES free-acid and 4.5 D-glucose (pH 7.4 adjusted with NaOH; 290 mosm/kg). The cell suspension was split into two aliquots. To one aliquot, 5 mM mannitol was added (0

glycine, control condition) and measurements were performed at 2-min intervals over 10 min. Thereafter, 5 mM glycine was added to the second aliquot and the cell volume was assessed over 40 min. In a second series of experiments, cells were exposed to an extracellular solution containing 5 mM glycine in absence of Na^+, which was prepared by iso-osmotic replacement of NaCl with choline-chloride. To assess dose-dependent effects of glycine on cell volume the cell suspension was divided into four aliquots and centrifuged for 5 min at $200\times g$. Immediately before the first measurement (time point 0) the pellets were resuspended in the extracellular solution containing 5 mM mannitol (0 mM glycine, control), or 0.3, 1, or 5 mM glycine (iso-osmotically replacing mannitol), respectively. Thereafter the samples were alternately measured every 5 min over 35 min. Flow cytometry was performed on a Cell Lab Quanta^{TM} SC flow cytometer (Beckman-Coulter). Mean cell volume (MCV in fl) was directly measured employing the Coulter principle for volume assessment, which is based on measuring changes in electrical resistance produced by nonconductive particles suspended in an electrolyte solution. The electronic volume channel was calibrated using 10-µm Flow-Check fluorospheres (Beckman-Coulter) by positioning this size bead in channel 200 on the volume scale. 8,000 single cells with a diameter $\geq$10 µm and $\leq$18 µm were analyzed per sample. Four independent experiments were performed per series.

Statistical analysis

Microsphere engulfment data are presented as mean ± SD (standard deviation). Statistical analysis was performed using SPSS 18.0. Each experiment was performed at least three times. In each experiment 100–200 cells were randomly evaluated. Student's double-sided *t* test for independent samples was applied to calculate levels of significance, $P < 0.05$ and $P < 0.01$. Patch clamp and flow cytometry data were analyzed with GraphPad Prism 6.0 software. Ordinary or repeated measures one-way ANOVA, paired or unpaired double-sided *t* tests were used as applicable. Experiments were repeated at least four times. Data are graphed as mean ± SEM (standard error of the means).

Results

Microglial cells express SNATs, but not GlyRs

Because the expression of GlyRs in monocyte-derived cells is controversial, we used RT-PCR analysis and electrophysiology to characterize potential glycine targets in microglial cells. In BV-2 cells as well as pMG, we did not detect any RT-PCR product for mRNA from GlyR1, GlyR2, GlyR3 or GlyR4. Interestingly, microglial cells revealed specific PCR products for the SNATs Slc38a1, Slc38a2, but not for Slc38a4 (Fig. 1).

Since activation of GlyR elicits a Cl^- conductance, whereas activation of SNAT induces a Na^+ conductance, we used a whole-cell perforated patch clamp technique to record glycine-induced changes in V_{mem} as well as ion currents in BV-2 cells. Application of glycine (5 mM) depolarized V_{mem} from -55.8 ± 4.5 to -20.3 ± 3.6 mV ($n = 14$; $P < 0.001$) and wash-out of glycine repolarized V_{mem} to -62.7 ± 8.1 mV ($n = 5$) (Fig. 2a, b). Furthermore, we identified a significant depolarization induced by 1 mM glycine ($n = 7$; $P < 0.05$), whereas addition of 0.3 mM glycine was yet without significant effect on V_{mem} ($n = 7$; $P = 0.14$) (Fig. 2d). In line with the depolarization of V_{mem}, glycine application activated an inward current of -19.2 ± 1.7 pA ($n = 7$), which was markedly suppressed upon withdrawal of glycine. The remaining current after wash-out of glycine was -2.0 ± 1.2 pA ($n = 6$) (Fig. 2a, c). To evaluate whether Na^+ is prerequisite for the glycine-induced changes of V_{mem} and inward current, we replaced Na^+ by choline in the extracellular saline. As shown in Fig. 2b, c, respectively, V_{mem} significantly repolarized to -58.7 ± 5.3 mV ($n = 7$; $P < 0.001$) and no significant inward current could be elicited (-2.1 ± 4.1 pA; $n = 4$; $P < 0.01$).

If glycine is transported into the cell, cell swelling is expected to be provoked due to an increase in intracellular osmolarity. Accordingly, we exposed BV-2 cells to glycine and quantified cell volume (CV) by flow cytometry. As shown in Fig. 3a, 5 mM glycine induced a clear shift in the

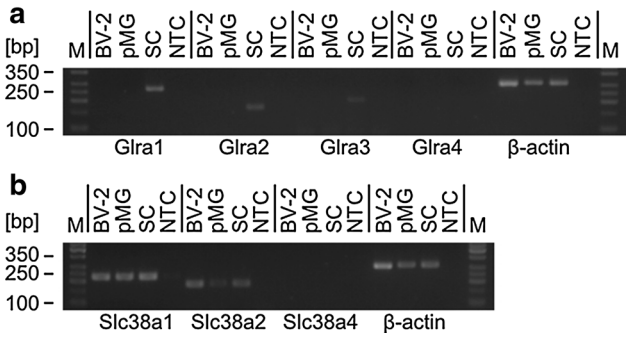

Fig. 1 RT-PCR analysis of glycine receptor (GlyR) and sodium-coupled neutral amino acid transporter (SNAT) alpha subunit isoforms in BV-2 cells, primary microglial cells (pMG), and spinal cord (SC). PCR products were obtained using specific primers to **a** mouse glycine receptor alpha subunit isoforms 1–4 (Glra1–4) and **b** mouse sodium-coupled amino acid transporters (members 1, 2 and 4 of solute carrier family 38; Slc38a1, 2 and 4). PCR products were separated on a 2 % agarose gel and visualized by Midori Green (NIPPON Genetics) staining. First and last lane contains standard DNA markers. (*bp* base pairs, *M* 50-bp size marker, *NTC* non-template control)

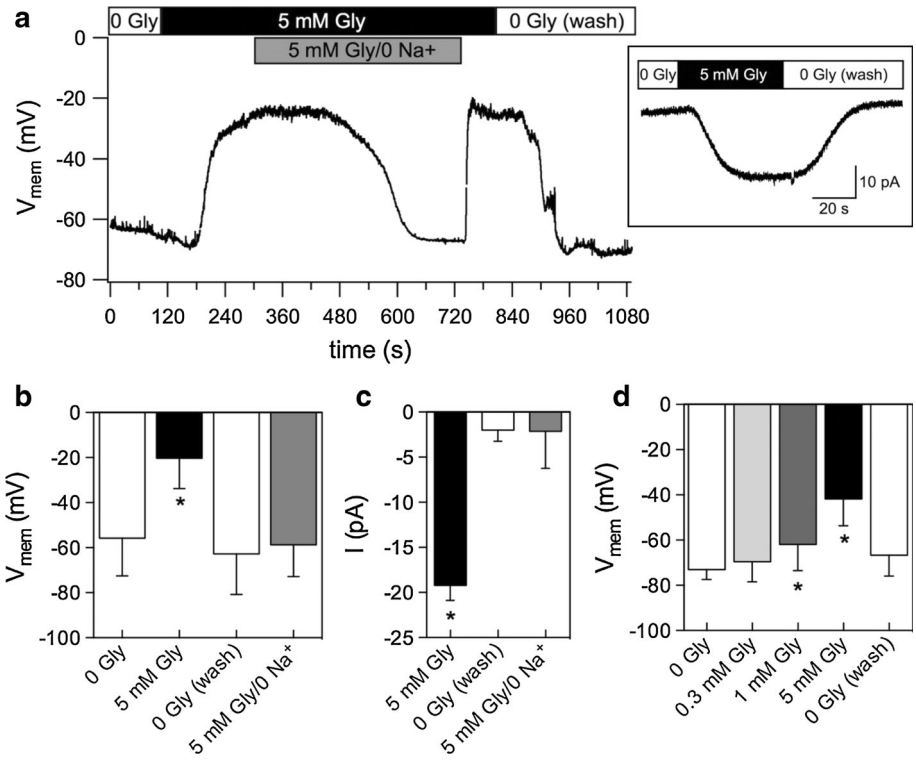

Fig. 2 Whole-cell perforated patch clamp recordings of cell membrane potential (V_{mem}) and SNAT-dependent Na^+ conductance. **a** Superfusion of BV-2 cells with glycine causes a sustained, reversible depolarization of V_{mem} paralleled by the activation of an inward current (*inset*). Glycine-induced depolarization and inward current were reversed by Na^+-free saline containing glycine. **b**–**d** Average changes in V_{mem} and inward current following superfusion with different concentrations of glycine. For nominally Na^+-free conditions (0 Na^+), NaCl was iso-osmotically replaced by choline-Cl. In each experimental conditions between 4 and 14 cells have been recorded. $^*P < 0.05$

frequency distribution of cell diameters towards higher values within 20 min. Figure 3b, showing the time course of glycine-induced cell swelling, demonstrates that after 20 min CV significantly increased from 1,660 ± 51 fl under control conditions to 1,839 ± 59 fl ($n = 4$; $P < 0.05$) in the presence of 5 mM glycine, which equals CV gain of ~9 %. As shown in Fig. 3c also 0.3 and 1.0 mM glycine provoked a significant increase in CV ($n = 5$, $P < 0.05$). Under nominally Na^+-free conditions no significant changes in CV are evident over time (Fig. 3b).

Thus, based on RT-PCR experiments, electrophysiological recordings and CV measurements, we conclude, similar to Schilling and Eder (2004), that glycine activates SNATs in microglial cells.

Glycine-dependent modulation of phagocytosis is related to SNAT

Because we have demonstrated in a previous study that phagocytosis and CV regulation share similarities (Harl et al. 2013) and in the present study that glycine provokes CV changes, we next evaluated the impact of glycine on phagocytosis. In a series of experiments, we compared whether amino acids in general and glycine specifically modulate phagocytosis in BV-2 cells. Accordingly, we maintained cells (1) in saline, (2) in DMEM, which, similar to blood serum, contained 0.4 mM glycine, and (3) saline containing glycine for 1 h (Fig. 4). In cells kept in saline, 62.85 ± 7.19 % contained at least one microsphere ($n = 17$ experiments; 3,272 cells in total). In cells cultured in DMEM, 68.18 ± 4.98 % contained at least one microsphere ($n = 6$ experiments; 1,264 cells in total). One hour exposure of BV-2 cells to 1 mM glycine increased the number of cells containing at least one microsphere by 13.44 ± 7.83 ($n = 6$ experiments; 1,212 cells in total).

Since we identified SNAT mRNA by RT-PCR products and an Na^+-dependent glycine-induced depolarization, we evaluated whether microsphere uptake is related to SNAT activation in BV-2 cells. In these phagocytosis experiments, we normalized the response for each experimental condition to that observed in saline. Incubation of BV-2 cells for 1 h in a nominally Na^+-free saline decreased phagocytosis by ~61 % compared to control conditions. Surprisingly, in Na^+-free extracellular saline, glycine increased phagocytosis by ~26 % compared to glycine-free Na^+-free extracellular saline. Exposure of BV-2 cells to MeAIB (10 mM) did not noticeably affect phagocytosis compared to control conditions. However, MeAIB suppressed glycine-dependent increase in uptake of microspheres (Fig. 4).

To test whether GlyRs were involved in phagocytosis in BV-2 cells, we evaluated whether the glycine-mediated effect was mimicked by taurine, suppressed by strychnine and whether it is depended on Cl^-. 1 mM glycine increased the number of cells containing at least one microsphere to ~113 % ($P < 0.05$; $n = 6$), whereas

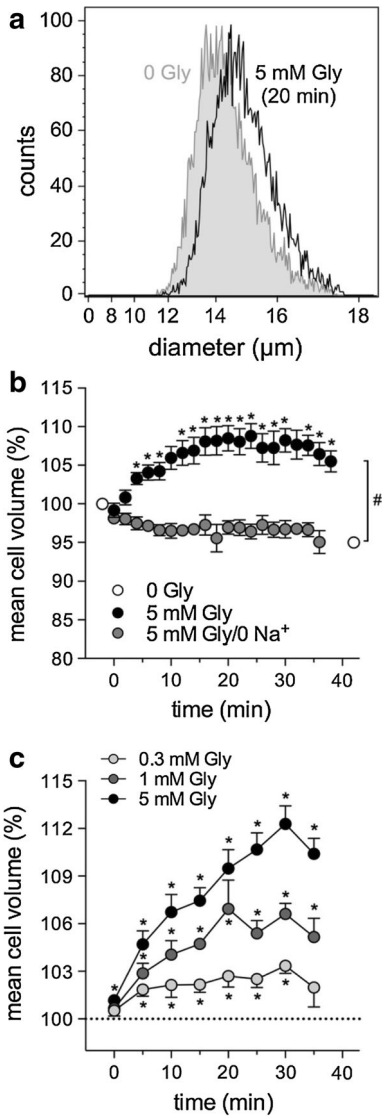

Fig. 3 Glycine increases cell volume in BV-2 cells in iso-osmotic conditions. Following addition of glycine, cell volume was measured using flow cytometry. **a** Histogram overlay shows a shift towards higher cell diameters after 20 min in presence of 5 mM glycine. **b** Comparisons of cell volume between 5 mM glycine containing solution and Na^+-free, 5 mM glycine containing solution. In presence of glycine, but absence of Na^+ (NaCl iso-osmotically replaced by choline-Cl), cell volumes remain unchanged over time, demonstrating an Na^+-dependency of glycine uptake. Cell volume data were analyzed by repeated measures ANOVA with a Dunnett post-test. $^*P < 0.05$; $^{\#}$significant difference ($P < 0.05$) to control values measured at the end of the experiment. Four independent experiments were performed *per* series. **c** Average cell volume at different glycine concentrations in relation to glycine-free solution plotted in dependence on different durations of glycine exposure. Data are shown as % of control values in the absence of glycine. Five independent experiments per concentration and duration of glycine exposure were performed. *Statistically significant difference ($P < 0.05$) to control values (0 mM glycine) at the respective time-points calculated by two-sided paired *t* tests

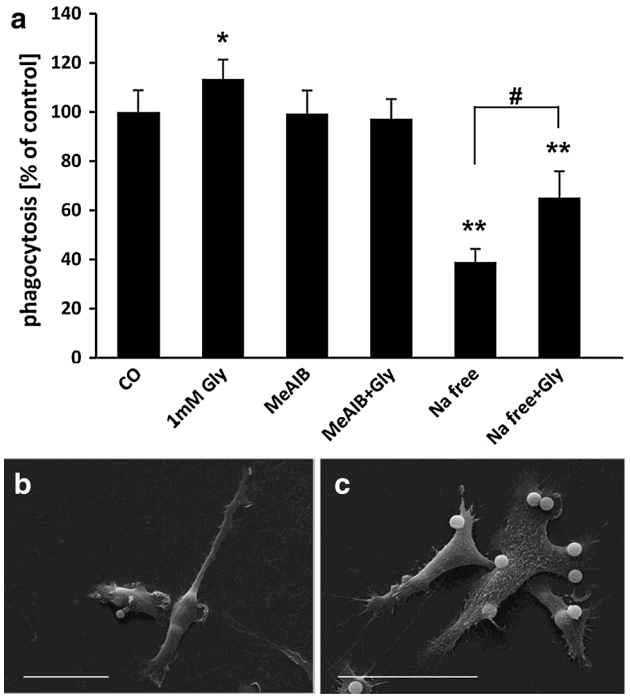

Fig. 4 Na^+- and SNAT-dependency of glycine-facilitated phagocytosis. Cells were exposed to microspheres (3.41×10^6 microspheres/2 ml solution) in different experimental conditions for 1 h. **a**: *Each bar* represents the mean ± SD of at least three independent experiments. In each experiment a total of about 600 cells have been evaluated. Incubation with 1 mM glycine (Gly) induced an increase in phagocytosis, that was absent after pre-incubation with MeAIB, a substrate of the SNAT, or by MeAIB alone. Phagocytosis significantly decreased after incubation in Na^+-free solution (Na free) in the absence and presence of 1 mM glycine. *Asterisks* (*, **) indicate $P < 0.05$ and $P < 0.01$, respectively, when compared with the control group, the rhombus (*hash*) indicates $P < 0.05$ when compared between Na^+-free solutions in the presence and absence of 1 mM glycine. Student's double-sided *t* test for independent samples was applied to calculate levels of significance. **b**, **c**: Representative images of microglial cells after 1 h incubation with microspheres using SEM. Cells incubated with 1 mM glycine co-applied to 10 mM MeAIB (**b**), and to Na^+-free solution (**c**). *Scale bars* 40 µM (**b**, **c**)

10 mM glycine failed to influence phagocytosis of microspheres (Fig. 5). Although glycine enhanced microsphere uptake, 1 mM taurine suppressed uptake of microspheres by ~15 %; whereas, 10 mM taurine increased uptake of microspheres by ~13 %. The number of cells containing at least one microsphere did not significantly differ between glycine and co-addition of glycine and strychnine (1 µM). The uptake of microspheres significantly decreased in nominally Cl^--free saline compared to control conditions. Administration of glycine to Cl^--free saline had no influence on the phagocytosis capability of BV-2 cells compared to Cl^--free saline alone (Fig. 5).

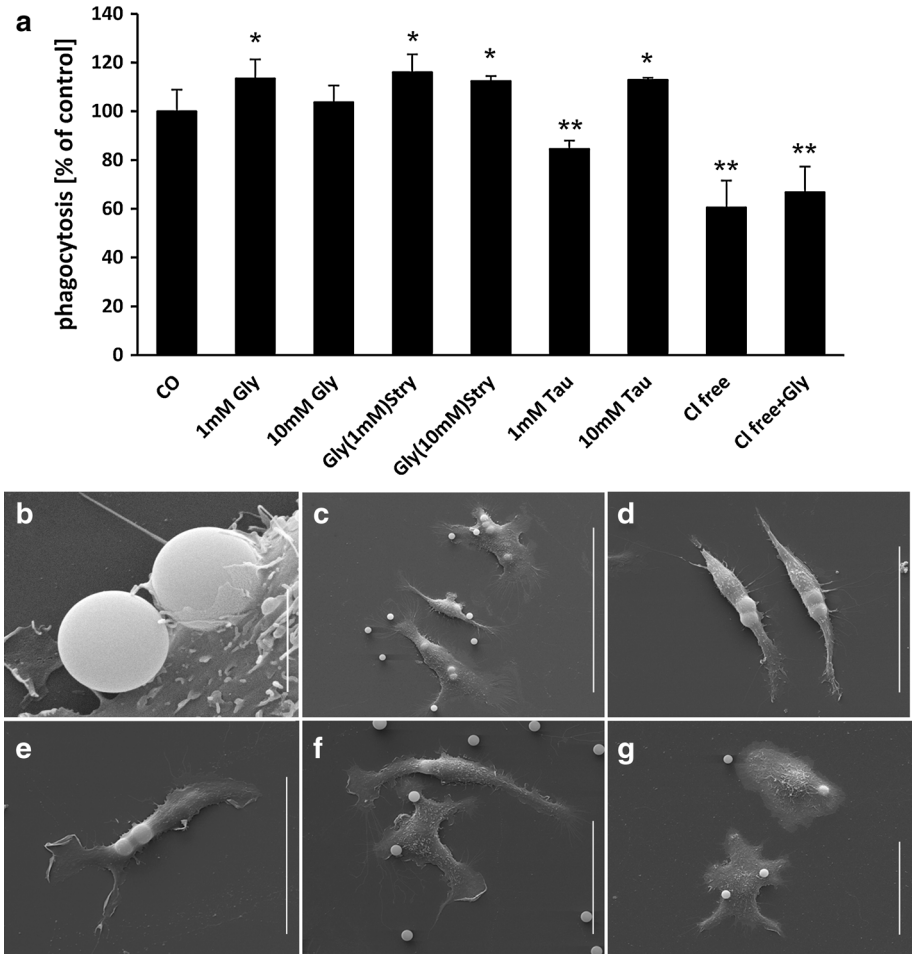

Fig. 5 Glycine-facilitated uptake of microspheres is GlyR-independent. BV-2 cells were exposed to polystyrene microspheres (3.41×10^6 microspheres/2 ml solution) for 1 h. Uptake of microspheres was evaluated using scanning electron microscopy. **a** Each *bar* represents the mean ± SD of at least three independent experiments. For each condition, about 600 cells have been evaluated. Glycine-facilitated phagocytosis is insensitive to 1 μM strychnine (Stry). Phagocytosis was suppressed after incubation with taurine (1 mM) and in Cl^--free extracellular solution in the absence and presence of 1 mM glycine. Student's double-sided *t* test for independent samples was applied to calculate levels of significance. *Asterisks* (*, **) indicate $P < 0.05$ and $P < 0.01$, respectively, when compared with the control group. **b** Representative image of microspheres attached to the surface of a microglial cell. Note the formation of engulfment pseudopodia, tightly embracing the right microsphere. **c**–**g** Representative images of microglial cells after incubation with microspheres for 1 h in saline (**c**), 1 mM glycine (**d**), 1 mM glycine co-incubated with 1 μM strychnine (**e**), 1 mM taurine (**f**), and after incubation in Cl^--free solution with 1 mM glycine (**g**). *Scale bars* 4 μM (**b**), 40 μM (**d**–**g**) and 100 μM (**c**)

Thus, similar to our RT-PCR analysis and electrophysiological experiments, the insensitivity to strychnine as well as opposite effects of glycine and taurine indicate that GlyR are not involved glycine-dependent effects on phagocytosis.

Glycine rescues phagocytosis in hypertonic conditions

Because glycine and SNATs are involved in regulatory volume increase, we next tested whether glycine affects phagocytosis in hypertonic conditions (DMEM; 400 mosmol/L). Microsphere uptake was quantified following hypertonic conditions for 6 and 12 h, respectively. Microspheres were added in the absence and presence of glycine (1 mM) in hypertonic conditions in the final hour. Following 6 or 12 h of hypertonic treatment, uptake of microspheres was decreased compared to isotonic conditions. However, when glycine was present in the final hour, the number of cells containing at least one microsphere were not different compared to isotonic conditions (Table 2).

Discussion

We have identified SNAT mRNA and glycine-activated Na^+ current in BV-2 cells, but did not detect mRNA for GlyRs mRNA. In line with these findings, microsphere

Table 2 Effect of hypertonicity and glycine on microsphere uptake in BV-2 cells

(a)	Relative phagocytosis (%)
Control	100.00 ± 7.30, $n = 6$
Hyper	89.23 ± 8.60, $n = 6$
5 h (hyper) + 1 h (1 mM Gly)	104.23 ± 3.30, $n = 3$
(b)	Relative phagocytosis (%)
Control	100.00 ± 7.98, $n = 4$
Hyper	81.26 ± 5.78, $n = 4^{*}$
11 h (hyper) + 1 h (1 mM Gly)	105.90 ± 6.95, $n = 3$

Cells were cultured in serum-free DMEM in normotonic or in hypertonic conditions (400 mosmol/L) for 6 h (a) or 12 h (b). In the final hour, cells were exposed to microspheres (3 µl/2 ml) in the absence or presence of glycine (1 mM). Phagocytosis was measured using SEM. Data are represented as mean ± SD and adapted to control = 100 %. Student's double-sided *t* test for independent samples was applied to calculate levels of significance

Asterisk (*) indicates $P < 0.05$ when compared with control group

uptake is suppressed by the SNAT inhibitor MeAIB, but not by the GlyR inhibitor, strychnine. The glycine-dependent increase in phagocytosis is detectable in normo- and hypertonic conditions.

GlyR and SNAT in monocyte-derived cells

Based on electrophysiological experiments, Schilling and Eder convincingly argued for the expression of SNATs but against the expression of GlyRs in BV-2 cells (Schilling and Eder 2004). These authors describe that (1) glycine depolarizes the membrane potential and induces an Na^+-dependent, but Cl^--independent ion current; (2) the glycine-induced current is suppressed by MeAIB, but not by strychnine; and (3) taurine does not induce an ion current. Using a perforated patch clamp technique, we confirmed that the glycine-induced current is sensitive to extracellular Na^+. We extended the electrophysiological experiments by RT-PCR analysis showing that BV-2 cells as well as pMG express Slc38a1 and Slc38a 2, but not GlyRs. Interestingly, peripheral monocyte-derived cells, like Kupffer cells, splenic and alveolar macrophages, express α- and β- subunit GlyR mRNA (Froh et al. 2002) and glycine-dependent modulation of intracellular Ca^{2+} is sensitive to strychnine, taurine, and extracellular Cl^- (Ikejima et al. 1996, 1997; Seabra et al. 1998; Wheeler and Thurman 1999). However, while the expression of mRNAs for the GlyR α-subunit and gephyrin, the protein that anchors the GlyR to cytoskeletal elements, were confirmed in rat peritoneal macrophages, functional glycine-mediated chloride currents in these cells could not be detected (Carmans et al. 2004).

SNATs are involved in phagocytosis

Recently, we described that suppression of Cl^- conductance inhibits phagocytosis in microglial cells (Harl et al. 2013). Because glycine causes a moderate increase in cell volume, glycine may affect phagocytosis by at least two ion currents. (1) The glycine-dependent increase in cell volume may activate a swelling-activated Cl^- conductance and (2) the transport of glycine by SNAT is associated with an Na^+ inward current. Thus, cell swelling due to influx of glycine and Na^+ as well as a possible RVD process due to activation of Cl^- conductance may modulate engulfment and uptake of particles. The balance between these volume regulatory processes could affect the magnitude of particle uptake. Glycine either decreases or does not affect phagocytosis of *E. coli* by blood monocytes (Spittler et al. 1999) or increases myelin uptake by peritoneal macrophages (Carmans et al. 2004). Interestingly, glycine-dependent increase in phagocytosis of myelin is insensitive to strychnine, but sensitive to the SNAT inhibitor 2-aminoisobutyric acid (AIB). Similarly, we show in the microglial cell line BV-2, that glycine-dependent increase in uptake of microspheres is related to SNAT. Whereas MeAIB eliminates the glycine effect, strychnine is ineffective. In line with this observation, we find that an Na^+ gradient is required because phagocytosis is reduced when Na^+ is replaced by choline.

Inflammatory processes are associated with hypertonicity (Brocker et al. 2012). At the cellular level, hyperosmotic stress induces expression of pro-inflammatory cytokines and decreases phagocytosis (Brocker et al. 2012; Lang et al. 2002; Németh et al. 2002; Otto et al. 2008; Pan et al. 2011; Warskulat et al. 1996, 1997). At the systemic pathophysiological level, diseases like, e.g., diabetes mellitus, asthma bronchiale or cystic fibrosis are associated with increased osmolarity as well as inflammatory processes (Brocker et al. 2012). In the brain, studies on rats demonstrate that experimentally increased ventricular osmolarity induces hydrocephalus (Kirshnamurthy et al. 2009) and neonatal hydrocephalus increases inflammation and microgliosis (Deren et al. 2010). In general, hypertonic stress causes up-regulation of osmoprotective genes, like betaine transporter or Na^+-myo-inositol cotransporter, which affects osmolyte levels in the brain (Bitoun and Tappaz 2000; Heilig et al. 1989; Ibsen and Strange 1996; Minami et al. 1996; Lien et al. 1990). Interestingly, osmolytes suppress the release of pro-inflammatory cytokines (Brocker et al. 2012), but increase phagocytosis (present study).

Regulation of extracellular glycine may affect physiology of neurotransmission and immune response in the brain. Glycine promotes inhibitory synaptic potentials (Dutertre et al. 2012) or enhances excitatory glutamatergic synaptic transmission via binding to NMDA-receptors (Thomson et al. 1989; Yang and Svensson 2008).

Critically, glycine transporters may either depress glutamatergic transmission by removing extracellular glycine or enhance glutamatergic transmission by delivering glycine by a reverse transport (Supplisson and Bergman 1997). In humans, non-ketotic hyperglycinemia is associated with severe neonate seizures (Lee 2011). Interestingly, glycine affects not only glutamatergic synaptic transmission, but also cell morphology. In a murine glycine transporter 1 knock out model, having higher levels of glycine in brain compared to wild-type animals, Bakker and colleagues observed an increased dendritic branching in hippocampal CA1 pyramidal cells compared to wild-type mice (Bakkar et al. 2011). If glycine transporters change the level of glycine in the vicinity of microglial cells, volume regulatory as well as membrane potential-dependent processes in microglia are affected. In previous studies, we demonstrated that changes in the concentration of the inorganic osmolyte Cl^-, affects phagocytosis and migration in microglia and are related to volume and ion regulatory processes (Furtner et al. 2007; Harl et al. 2013; Zierler et al. 2008). The results in the present study attribute similar functions to glycine, an important organic osmolyte.

In conclusion, we have identified a SNAT-dependent mechanism by which glycine facilitates phagocytosis. The glycine-dependent increase in phagocytosis may be particularly relevant in hypertonic conditions, which are associated with inflammatory processes. As suggested by Schilling and Eder (2004), an increase in glycine required to activate SNAT may be a consequence of release of intracellular glycine from dying cells following traumata or ischemia. Thus, an increase in extracellular glycine could increase phagocytosis leading to removal of pathogens or cell debris and, accordingly, decrease inflammatory processes. In addition, microglial cells might contribute to the clearance of brain interstitial fluid from excess glycine in the vicinity of damaged cells. Because glycine has anti-inflammatory and immunomodulatory properties (Wang et al. 2013), daily nutritional uptake of glycine may have important consequences in health and disease (Wu 2013; Wu et al. 2013).

Acknowledgments We thank Dr. Karin Oberascher for help in cell culture procedures and Dr. Wolf-Dietrich Krautgartner for providing access to the scanning electron microscope. This project was supported by the PMU grant R-11/02/024-JAK to MJ.

Conflict of interest The authors declare no conflict of interest.

References

Bakkar W, Ma CL, Pabba M, Khacho P, Zhang YL, Muller E, Martina M, Bergeron R (2011) Chronically saturating levels of endogenous glycine disrupt glutamatergic neurotransmission and enhance synaptogenesis in the CA1 region of mouse hippocampus. Synapse 65:1181–1195

Bitoun M, Tappaz M (2000) Gene expression of taurine transporter and taurine biosynthetic enzymes in brain of rats with acute or chronic hyperosmotic plasma. A comparative study with gene expression of myo-inositol transporter, betaine transporter and sorbitol biosynthetic enzyme. Mol Brain Res 77:10–18

Brocker C, Thompson DC, Vasiliou V (2012) The role of hyperosmotic stress in inflammation and disease. Biomol Concept 3:345–364

Carmans S, Hendriks JJ, Thewissen K, Van den Eynden J, Stinissen P, Rigo JM, Hellings N (2004) The inhibitory neurotransmitter glycine modulates macrophage activity by activation of neutral amino acid transporters. J Neurosci Res 88:2420–2430

Deren KE, Packer M, Forsyth J, Milash B, Abdullah OM, Hsu EW, McAllister JP 2nd (2010) Reactive astrocytosis, microgliosis and inflammation in rats with neonatal hydrocephalus. Exp Neurol 226:110–119

Dutertre S, Becker C-M, Betz H (2012) Inhibitory glycine receptors: an update. J Biol Chem 287:40216–40223

Franchi-Gazzola R, Dall'Asta V, Sala V, Visigalli R, Bevilacqua E, Gaccioli F, Gazzola GC, Bussolati O (2006) The role of the neutral amino acid transporter SNAT2 in cell volume regulation. Acta Physiol 187:273–283

Froh M, Thurman RG, Wheeler MD (2002) Molecular evidence for a glycine-gated chloride channel in macrophages and leukocytes. Am J Physiol 283:G856–G863

Furtner T, Zierler S, Kerschbaum HH (2007) Blockade of chloride channels suppresses engulfment of microspheres in the microglial cell line, BV-2. Brain Res 1184:1–9

Harl B, Schmölzer J, Jakab M, Ritter M, Kerschbaum HH (2013) Chloride channel blockers suppresses formation of engulfment pseudopodia in microglial cells. Cell Physiol Biochem 31:319–337

Heilig CW, Stromski ME, Blumenfeld JD, Lee JP, Gullans SR (1989) Characterization of the major brain osmolytes that accumulate in salt-loaded rats. Am J Physiol 257:F1108–F1116

Hoffmann OM, Becker D, Weber JR (2007) Bacterial hydrogen peroxide contributes to cerebral hyperemia during early stages of experimental pneumococcal meningitis. J Cereb Blood Flow Metab 27:1792–1797

Hoffmann EK, Lambert IH, Pedersen SF (2009) Physiology of cell volume regulation in vertebrates. Physiol Rev 89:193–227

Horwitz LD, Kaufman D, Keller MW, Kong Y (1994) Time course of coronary endothelial healing after injury due to ischemia and reperfusion. Circulation 90:2439–2447

Ibsen L, Strange K (1996) In situ localization and osmotic regulation of the Na(+)-myo-inositol cotransporter in rat brain. Am J Physiol 271:F877–F885

Ikejima K, Iimuro Y, Forman DT, Thurman RG (1996) A diet containing glycine improves survival in endotoxin shock in the rat. Am J Physiol 271:G97–G103

Ikejima K, Qu W, Stachlewitz RF, Thurman RG (1997) Kupffer cells contain a glycine-gated chloride channel. Am J Physiol 272:G1581–G1586

Kirshnamurthy S, Li J, Schultz L, McAllister JP 2nd (2009) Intraventricular infusion of hyperosmolar dextran induces hydrocephalus: a novel animal model of hydrocephalus. Cerebrospinal Fluid Res 11:16

Kreutzberg GW (1996) Microglia: a sensor for pathological events in the CNS. Glia 19:312–318

Lang F, Ritter M, Völkl H, Häussinger D (1993) The biological significance of cell volume. Renal Physiol Biochem 16:48–65

Lang F, Busch GL, Ritter M, Völkl H, Waldegger S, Gulbins E, Häussinger D (1998) Functional significance of cell volume regulatory mechanisms. Physiol Rev 78:247–306

Lang KS, Fillon S, Schneider D, Rammensee HG, Lang F (2002) Stimulation of TNF alpha expression by hyperosmotic stress. Pflügers Arch 443:798–803

Lee W-T (2011) Disorders of amino acid metabolism associated with epilepsy. Brain Dev 33:745–752

Lien YH, Shapiro JI, Chan L (1990) Effects of hypernatremia on organic brain osmoles. J Clin Invest 85:1427–1435

Mackenzie B, Erickson JD (2004) Sodium-coupled neutral amino acid (System N/A) transporters of the SLC38 gene family. Pflügers Arch 447:784–795

Mikalauskas S, Mikalauskiene L, Bruns H, Nickkholgh A, Hoffmann K, Longerich T, Strupas K, Büchler MW, Schemmer P (2011) Dietary glycine protects from chemotherapy-induced hepatotoxicity. Amino Acids 40:1139–1150

Minami Y, Inoue K, Shimada S, Morimura H, Miyai A, Yamauchi A, Matsunaga T, Tohyama M (1996) Rapid and transient up-regulation of Na^+/myo-inositol cotransporter transcription in the brain of acute hypernatremic rats. Brain Res Mol Brain Res 40:64–70

Németh ZH, Deitch EA, Szabó C, Haskó G (2002) Hyperosmotic stress induces nuclear factor-kappaB activation and interleukin-8 production in human intestinal epithelial cells. Am J Pathol 161:987–996

Otto NM, Schindler R, Lun A, Boenisch O, Frei U, Oppert M (2008) Hyperosmotic stress enhances cytokine production and decreases phagocytosis in vitro. Crit Care 12:R108

Pan Z, Wang Z, Yang H, Zhang F, Reinach PS (2011) TRPV1 activation is required for hypertonicity-stimulated inflammatory cytokine release in human corneal epithelial cells. Investig Ophthalmol Vis Sci 52:485–493

Schemmer P, Bradford BU, Rose ML, Bunzendahl H, Raleigh JA, Lemasters JJ, Thurman RG (1999) Intravenous glycine improves survival in rat liver transplantation. Am J Physiol 276:G924–G932

Schilling T, Eder C (2004) A novel physiological mechanism of glycine-induced immunomodulation: Na^+-coupled amino acid transporter currents in cultured brain macrophages. J Physiol 559:35–40

Schiöth HB, Roshanbin S, Hägglund MG, Fredriksson R (2013) Evolutionary origin of amino acid transporter families SLC32, SLC36 and SLC38 and physiological, pathological and therapeutic aspects. Mol Aspects Med 34:571–585

Schliess F, Häussinger D (2003) Cell volume and insulin signalling. Inter Rev Cytol 225:187–228

Seabra V, Stachlewitz RF, Thurman RG (1998) Taurine blunts LPS-induced increases in intracellular calcium and TNF-α production by Kupffer cells. J Leukoc Biol 64:615–621

Spittler A, Reissner CM, Oehler R, Gornikiewicz A, Gruenberger T, Manhart N, Brodowicz T, Mittlboeck M, Boltz-Nitulescu G, Roth E (1999) Immunomodulatory effects of glycine on LPS-treated monocytes: reduced TNF-α production and accelerated IL-10 expression. JASEB 13:563–571

Stoffels B, Türler A, Schmidt J, Nazir A, Tsukamoto T, Moore BA, Schnurr C, Kalff JC, Bauer AJ (2011) Anti-inflammatory role of glycine in reducing rodent postoperative inflammatory ileus. Neurogastroenterol Motil 23:76–87

Supplisson S, Bergman C (1997) Control of NMDA receptor activation by a glycine transporter co-expressed in Xenopus oocytes. J Neurosci 17:4580–4590

Thomson AM, Walker VE, Flynn DM (1989) Glycine enhances NMDA-receptor mediated synaptic potentials in neocortical slices. Nature 338:422–424

Thurman RG, Zhong Z, von Frankenberg M, Stachlewitz RF, Bunzendahl H (1997) Prevention of cyclosporin-induced nephrotoxicity with dietary glycine. Transplantation 63:1661–1667

Tramacere M, Petronini PG, Severini A, Borghetti AF (1984) Osmoregulation of amino acid transport activity in cultured fibroblasts. Exp Cell Res 151:70–79

Van den Eynden J, Notelaers K, Brône B, Janssen D, Nelissen K, Sahebali S, Smolders I, Hellings N, Steels J, Rigo JM (2011) Glycine enhances microglial intracellular calcium signaling. A role for sodium-coupled neutral amino acid transporters. Pflügers Arch 461:481–491

Wang W, Wu Z, Dai Z, Yang Y, Wang J, Wu G (2013) Glycine metabolism in animals and humans: implications for nutrition and health. Amino Acids 45:463–477

Warskulat U, Zhang F, Häussinger D (1996) Modulation of phagocytosis by anisoosmolarity and betaine in rat liver macrophages (Kupffer cells) and RAW 264.7 mouse macrophages. FEBS Lett 391:287–292

Warskulat U, Wettstein M, Häussinger D (1997) Osmoregulated taurine transport in H4IIE hepatoma cells and perfused rat liver. J Biochem 1:683–690

Wheeler MD, Thurman RG (1999) Production of superoxide and TNF-α from alveolar macrophages is blunted by glycine. Am J Physiol 277:L952–L959

Wheeler MD, Ikejima K, Enomoto N, Stachlewitz RF, Seabra V, Zhong Z, Yin M, Schemmer P, Rose ML, Rusyn I, Bradford B, Thurman RG (1999) Glycine: a new anti-inflammatory immunonutrient. Cell Mol Life Sci 56:843–856

Wu G (2013) Functional amino acids in nutrition and health. Amino Acids 45:407–411

Wu G, Wu Z, Dai Z, Yang Y, Wang W, Liu C, Wang B, Wang J, Yin Y (2013) Dietary requirements of "nutritionally non-essential amino acids" by animals and humans. Amino Acids 44:1107–1113

Yancey PH (2005) Organic osmolytes as compatible, metabolic and counteracting cytoprotectants in high osmolarity and other stresses. J Exp Biol 208:2819–2830

Yang CR, Svensson KA (2008) Allosteric modulation of NMDA receptor via elevation of brain glycine and D-serine: the therapeutic potentials for schizophrenia. Pharmacol Ther 120:317–332

Zhong Z, Arteel GE, Connor HD, Yin M, Frankenberg MV, Stachlewitz RF, Raleigh JA, Mason RP (1998) Cyclosporin A increases hypoxia and free radical production in rat kidneys: prevention by dietary glycine. Am J Physiol 275:F595–F604

Zierler S, Frei E, Grissmer S, Kerschbaum HH (2008) Chloride influx provokes lamellipodium formation in microglial cells. Cell Physiol Biochem 21:55–62